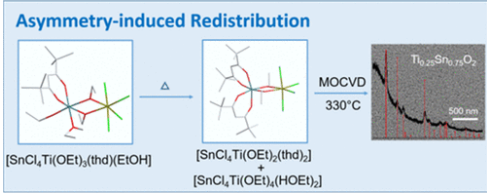


Sl. No.	<p style="text-align: center;">IIT Ropar List of Recent Publications with Abstract Coverage: December, 2021</p>
1.	<p>A Device to Reduce Vasovagal Syncope in Blood Donors R Kumar, AK Sahani - 43rd Annual International Conference of the IEEE Engineering in Medicine & Biology Society, 2021</p> <p>Abstract: Vasovagal Syncope (VVS), or the transient loss of consciousness is the most widely recognized reason for syncope. (VVS), is a typical dysfunction of the autonomic nervous system. There are various factors which can influence the syncope. The major classification of the syncope are reflex(neurally mediated) syncope, syncope due to orthostatic hypertension, Cardiac syncope(cardiovascular). The vasovagal syncope is the part of reflex (neurally mediated)syncope, there are various cause of vasovagal reactions but in blood donation it is mediated due to the pooling of blood at calf muscles. Such near syncope incidence while donating the blood or after donation hampers the future motivation for blood donation of the donors. In this paper, we developed an electronic massager for calf muscles that can reduce the risk of VVS. It has a programmable circuit which can control the vacuum pump so that it can inflate and deflate the cuffs synergistically. The massager can relax the blood donor thereby reducing apprehension prior to blood donation and thus diverting from the trigger of Phlebotomy and improve peripheral blood circulation thereby improving venous return to the heart. This is expected to reduce the risk of VVS.</p>
2.	<p>A hyperelastic model to capture the mechanical behaviour and histological aspects of the soft tissues KK Dwivedi, P Lakhani, S Kumar, N Kumar - Journal of the Mechanical Behavior of Biomedical Materials, 2021</p> <p>Abstract: It is well established that the soft connective tissues show a nonlinear elastic response that comes from their microstructural arrangement. Tissues' microstructure alters with various physiological conditions and may affect their mechanical responses. Therefore, the accurate prediction of tissue's mechanical response is crucial for clinical diagnosis and treatments. Thus, a physically motivated and mathematically simplified model is required for the accurate prediction of tissues' mechanical and structural responses. This study explored the 'Exp-Ln' hyperelastic model (Khajehsaeid et al., 2013) to capture soft tissues' mechanical and histological behaviour. In this work, uniaxial tensile test data for the belly and back pig skin were extracted from the experiments performed in our laboratory, whereas uniaxial test data for other soft tissues (human skin, tendon, ligament, and aorta) were extracted from the literature. The 'Exp-Ln; and other hyperelastic models (e.g. Money Rivlin, Ogden, Yeoh, and Gent models) were fitted with these experimental data, and obtained results were compared between the models. These results show that the 'Exp-Ln' model could capture the mechanical behaviour of soft tissues more accurately than other hyperelastic models. This model was also found numerically stable for all modes and ranges of deformation. This study also investigated the link between 'Exp-Ln' material parameters and tissue's histological parameters. The histological parameters such as collagen content, fibre free length, crosslink density, and collagen arrangement were measured using staining and ATR-FTIR techniques. The material parameters were found statistically correlated with the histological parameters. Further, 'Exp-Ln' model was implemented in ABAQUS through the VUMAT subroutine, where the mechanical behaviour of various soft tissues was simulated for different modes of deformation. The finite element analysis results obtained using the 'Exp-Ln' model agreed with the experiments and were more accurate than other hyperelastic models. Overall, these results demonstrate the capability of 'Exp-Ln' model to predict the mechanical and structural responses of the soft tissues.</p>

3.	<p>A modified approach to determine suspended sediment transport effectiveness in Indian rivers S Maheshwari, SR Chavan - Journal of Hydrology, 2021</p> <p>Abstract: Transport Effectiveness (TE) of a discharge is defined as the product of the frequency of discharge and corresponding sediment transport rate. Maximization of TE function helps in finding the “effective discharge (Q_e)” which is responsible for the transfer of the majority of sediments over a prolonged period. This approach to determine Q_e is famously known as Magnitude-Frequency Analysis (MFA). Conventionally, MFA involves the construction of the TE function by assuming (i) a location-specific probability density function (PDF) for discharge and (ii) power-law relationship between discharge and sediment transport rate. There have been attempts in the past to derive expressions for Q_e by assuming positively skewed PDFs for discharge. The present study proposes a modified approach to estimate TE-based Q_e for general discharge distribution datasets which alleviates the limitation of assuming a location-specific PDF. The approach involves the transformation of discharge data through Box-Cox transformation and subsequently performing MFA to determine Q_e. An expression for the analytical solution of TE-based Q_e is derived for the proposed framework of MFA. The robustness of the approach is established through a simulation study by generating discharge data using lognormal, Gamma, and log Pearson type III distributions. In this study, the influence of the hysteresis effect was investigated for total as well as seasonal datasets according to the considerations of the rising and falling stages for 14 stream gauges in South Indian Rivers. The analysis is performed by using the suspended sediment load and discharge data whereas the bedload has been excluded. Subsequently, the estimates of Q_e based on the proposed approach () were computed considering various sediment rating curves fitted for total, seasonal, stage and season-stage based datasets. Finally, the variation of with various catchment descriptors was examined.</p>
4.	<p>A QoS-aware Routing based on Bandwidth Management in Software-Defined IoT Network P Kamboj, S Pal, A Mehra - 18th International Conference on Mobile Ad Hoc and Smart Systems, 2021</p> <p>Abstract: The burgeoning demands of the Internet of Things (IoT) applications such as video/audio streaming in surveillance, disaster recovery, multimedia, and healthcare paves the need to provide better Quality of Service (QoS) delivery. The growth in the amount of data generated by multimedia applications increases congestion in the network. Software-Defined Networking (SDN) is an emerging approach that centrally controls the network and solves the congestion problem in the network. SDN has many advantages that help in network management, traffic shaping, and routing in the IoT network to manage the data generated from a diverse range of applications. In this paper, we propose a congestion technique using Hierarchical Token Bucket (HTB) to manage the bandwidth in the Software-Defined IoT (SDIoT) network. Further, we propose a routing scheme to compute optimal routing shortest paths using Dijkstra’s algorithm by selecting the min-cost path based on the priorities of traffic flows. The results illustrate that the proposed approach achieves a reduction in end-to-end delay by 38%, 44% and higher average throughput by 29%, 43% in comparison with the benchmark schemes - SDN with HTB and the Delay Minimization method, respectively.</p>
5.	<p>An Approach for Identifying and Customizing the Effective Ecodesign Tools for Environmentally Sustainable Product Development PK Singh, P Sarkar - ASME International Design Engineering Technical Conferences and Computers and Information in Engineering Conference, 2021</p> <p>Abstract: Producing environmentally benign products has now become one of the key challenges of companies across the globe. It can be achieved by utilizing the ecodesign tools in product</p>

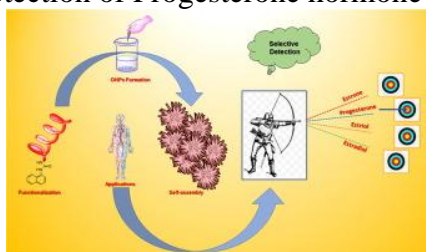
	<p>development process for reducing the environmental impact of products during the design stage itself. Although, the ecodesign tools are available in abundance but there is a lack of studies that can help companies to identify suitable tools. A novel approach has been developed in this study which assists companies to identify and adopt effective ecodesign tools. In this study, three companies related to different product categories are included for testing the proposed approach. Results show that ‘Ecodesign Checklist,’ ‘Material, Energy, Toxicity (MET) Matrix’ and ‘Life Cycle Design Strategy (LiDS) Wheel’ are the three most effective ecodesign tools among the tested tools. Also, it is realized that if these three ecodesign tools are customized and integrated together in a specific sequence then it can be used by the designers, especially novice designers, as an ecodesign methodology. This methodology has the potential to guide designers in the form of a step by step approach during environmentally conscious product development.</p>
6.	<p>An Intrusion Detection System on Fog Architecture M Sahi, M Soni, N Auluck - IEEE 18th International Conference on Mobile Ad Hoc and Smart Systems, 2021</p> <p>Abstract: Due to advancements in technology, electrical appliances are now inter-connected. The goal of Internet -of-things (IoT) is to access every appliance or device through the Internet. This is done in order to operate these gadgets from remote locations. The goal is to improve our day-to-day life. However, this technology raises serious privacy and security issues. As IoT devices are resource-constrained, it is impractical to secure them using traditional approaches. Hence, a light-weight Intrusion detection system (IDS) is required. In this work, we implement a machine learning based Network Intrusion Detection (NID) system in a multi-node fog environment using a Raspberry Pi cluster on a local area network. The proposed Pi-IDS system has been evaluated on ADFA-LD datasets. These datasets comprise of new generation system calls for various attacks on different applications. The proposed fog architecture offers significant advantages in terms of latency, energy consumption and cost over traditional cloud or dedicated personal computer systems. The experiments show that we are able to achieve a Recall of 89% in ADFA-LD with the XGBoost model. The proposed system was able to predict intrusion with an inference time 130 ms in comparison to Cloud with 735 ms, with an estimated running cost of 201 INR/month in comparison to the Cloud cost of 2051 INR/month.</p>
7.	<p>Analysis and Mitigation of Common Mode Noise in Three-Phase SiC-Based Brushless DC Motor Drive with 120 Conduction Mode S Singh, NBY Gorla, K Jayaraman, J Pou - IEEE Transactions on Power Electronics, 2021</p> <p>Abstract: The generation and propagation of common mode (CM) noise depends on the pulsewidth modulation (PWM) technique, parasitic capacitances, and rate of change of voltages imposed on the motor. In the literature, the CM noise analysis of the BLdc drive operated with 120 conduction mode is reported neglecting the impact of the floating phase, and the analysis is restricted to low-voltage silicon-based drives. In this paper, an in-depth theoretical analysis of the CM noise in BLdc drive is presented considering two commonly used schemes in 120 conduction mode, (i) six-step commutation (SSC) and (ii) bipolar PWM (BPWM). It is proven through experiments that the impact of the floating phase cannot be neglected especially with the high voltage slew rate imposed by silicon carbide (SiC) based inverters on the drives. By Considering the impact of floating phase, the CM noise in BLdc drive is modelled through mathematical equations and suitable equivalent circuits are presented. Finally, a step-by-step design procedure of the CM filter for BLdc drive is presented. Experimental results on a three-phase star-connected SiC-based BLdc drive are provided to substantiate the analysis and CM filter design.</p>

8.	<p>Analysis and Modeling of Activity-Selection Behavior in Collaborative Knowledge-Building A Chhabra, SRS Iyengar, JS Saini, V Malik - Transactions on Computational Collective Intelligence XXXVI: Part of the Lecture Notes in Computer Science book series, 2021</p> <p>Abstract: People neither behave uniformly in their social lives nor is their behavior entirely arbitrary. Rather, their behavior depends on various factors such as their skills, motives, and backgrounds. Our analysis shows that such a behavior also prevails in the websites of Stack Exchange. We collect and analyze the data of over 5.3 million users from 156 Stack Exchange websites. In these websites, users' diverse behavior shows up in the form of different activities that they choose to perform as well as how they stimulate each other for more contribution. Using the insights gained from the empirical analysis as well as the classical cognitive theories, we build a general cognitive model depicting the users' interaction behavior emerging in collaborative knowledge-building setups. Further, the analysis of the model indicates that for any given collaborative system, there is an optimal distribution of users across its activities that leads to the maximum knowledge generation. We also apply the model on Stack Exchange websites and identify the under-represented activities.</p>
9.	<p>Anisotropic electrical conduction on ion induced nanorippled CoSi surface BK Parida, A Kundu, KS Hazra, S Sarkar - Applied Physics A, 2021</p> <p>Abstract: We investigate electrical conduction on ion-induced nanorippled $\text{Co}_{0.69}\text{Si}_{0.31}$ surfaces. Oblique Ar^+ ion bombardment performed by varying the ion fluence within 1.12×10^{18}–6.73×10^{18} ions cm^{-2} showed well-ordered ripples aligned perpendicular to the ion beam direction. At higher fluence, hillock like structures evolve due to shadowing effect. Electrical measurements on the pristine and patterned surfaces show strong dependency on the patterning of the surface. Channel resistance is found to be highly dependent on ripple amplitude, and therefore, an anisotropy in electrical response along two orthogonal directions of the sample surface is evident due to the difference in effective channel length as a consequence of ripple formation. The surface resistance is found to be dependent on the ripple amplitude of the patterned surface. The present ion irradiation based post processing of the grown films present a unique approach towards a systematic improvement in electrical conduction.</p>
10.	<p>Assessment of positional error and hole quality during vibration-based drilling of aerospace alloy M Singh, S Dhiman, H Singh, CC Berndt - Journal of Mechanical Science and Technology, 2021</p> <p>Abstract: Modulation assisted drilling (MAD) superimposes low frequency (< 1000 Hz) and high amplitude (< 150 μm) vibrations to the cutting tool, more specifically to the drill bit in the feed direction during drilling. The present work investigates the effect of low-frequency vibrations on the drilled holes quality during MAD for nickel-based superalloy, Inconel-718 as work material. The vibrations were superimposed on the drill bit using a specialized tool holder (TriboMAM, a piezoelectric driven patented device). Quality comparison of conventionally and modulated-assisted drilled holes was done on the basis of positional error by a novel approach. As per the discrete chip production model during MAD, a rotational speed of 2200, the modulation frequency of 220 Hz, amplitude of 0.008 mm, and feed rate of 0.031 mm/rev led to a reduction in positional error, thrust force and torque by 52 %, 11 %, and 32 %, respectively, in comparison with the CD. MAD due to its intermittent cutting nature, results in a better lubricant flow during the operation, and production of finer chips; both factors help to reduce frictional heat, tool wear and thrust force. These attributes, in turn help to achieve less positional error. Moreover, the cyclic drilling force also contributes to reduce thrust force as well as positional error due to hammering action. Thus, the results of the study indicate that MAD is a better contender for quality-oriented machining of the given superalloy within the chosen parametric domain following the discrete cutting model.</p>

11.	<p>Assessment of temporal change in the tails of probability distribution of daily precipitation over India due to climatic shift in 1970s N Gupta, SR Chavan - Journal of Water and Climate Change, 2021</p> <p>Abstract: Daily precipitation extremes are crucial in the hydrological design of major water control structures and are expected to show a changing tendency over time due to climate change. The magnitude and frequency of extreme precipitation can be assessed by studying the upper tail behavior of probability distributions of daily precipitation. Depending on the tail behavior, the distributions can be classified into two categories: heavy-tailed and light-tailed distributions. Heavier tails indicate more frequent occurrences of extreme precipitation events. In this paper, we have analyzed the temporal change in the tail behavior of daily precipitation over India from pre- to post-1970 time periods as per the global climatic shift. A modified Probability Ratio Mean Square Error norm is used to identify the best-fit distribution to the tails of daily precipitation among four theoretical distributions (e.g., Pareto-type II, Lognormal, Weibull, and Gamma distributions). The results indicate that the Lognormal distribution, which is a heavy-tailed distribution, fits the tails of daily precipitation for the majority of the grids. It is inferred from the study that there is an increase in the heaviness of tails of daily precipitation data over India from pre- to post-1970 time periods.</p>
12.	<p>Asymmetry-Induced Redistribution in Sn (IV)–Ti (IV) Hetero-Bimetallic Alkoxide Precursors and Its Impact on Thin-Film Deposition by Metal–Organic Chemical Vapor Deposition S Mishra, E Jeanneau, L Tian, I Nuta, E Blanquet... R Ahuja... - Crystal Growth & Design, 2021</p> <p>Abstract: With an aim to enhance the stability and volatility of the heterometallic derivative $[\text{SnCl}_4(\mu\text{-OEt})_2\text{Ti}(\text{OEt})_2(\text{HOEt})_2]$ (A), obtained conveniently and quantitatively as a simple adduct formula from the equivalent reaction of commercially available SnCl_4 and $\text{Ti}(\text{OEt})_4$ in toluene/ethanol, its modification with 2,2,6,6-tetramethyl-3,5-heptanedione (thdH) is reported. The modified precursor $[\text{SnCl}_4(\mu\text{-OEt})_2\text{Ti}(\text{thd})(\text{OEt})(\text{HOEt})]$ (1), obtained from an equimolar reaction of A and thdH, is stable at room temperature but rearranges on heating into A and $[\text{SnCl}_4(\mu\text{-OEt})_2\text{Ti}(\text{thd})_2]$ (2), as confirmed by vapor pressure measurements and density functional theory calculations. The heterometallic 2 can be obtained in excellent yield from the reaction of A and thdH in a 1:2 molar ratio and is stable in the solid and solution phase up to 200 °C. However, the asymmetric nature of its structure consisting of fragments of titanium β-diketonate and tin chloride connected by bridging ethoxo groups leads to its breakdown into two homometallic components in the gas phase, leading to the deposition of tin-rich metal oxide films on the substrate.</p> 
13.	<p>Backbone Extension via Peptidomimetics at N-terminal; Self-assembled Nanofibrous Cluster and Application to Selective Progesterone Detection in an Aqueous medium S Saini, N Kaur, N Singh - Spectrochimica Acta Part A: Molecular and Biomolecular Spectroscopy, 2021</p> <p>Abstract: Despite the adequacy of the endogenous steroid (progesterone) levels in biological functioning, elevated levels of progesterone hormone have several physiological effects that are amplified due to its direct and indirect uptake from the environment, food products, and medical therapy. So, it is much needed to evaluate the progesterone levels in environmental samples as well as for biological fluids. In this work, we focused on the development of the nano sensing probe for</p>

the selective detection of progesterone among the library of steroid hormones belonging to the class of female sex hormones. Herein, functionalization of dipeptide is carried out at N-terminal to produce N-functionalized dipeptide (SS3), and simultaneously, its self-assembly properties are explored. Furthermore, HR-TEM imaging was also performed to examine the morphology of the self-assembled architectures before and after the addition of the steroid hormone. To investigate the binding mechanism of the sensing probe, Fluorescence spectroscopy, Circular Dichroism (CD), MD-Simulation, and DFT studies were performed and studied in detail. Moreover, to check the potency of the real-time application of the developed nanoprobe, we have successfully determined the spiked concentration of progesterone levels in pharmaceutical and biological fluid samples with functional percentage recovery. Also, the stability and other competitive binding studies of the probe with the coexisting substances are performed to check the rationality of the sensing probe at physiological conditions.

Graphical Abstract: Urea-functionalization of dipeptide molecule at N-terminal is carried out and its self-assembly properties are explored. Simultaneously, the functionalized dipeptide used as sensing probe for the selective detection of Progesterone hormone in an aqueous media.



[Biomimetic nanofiltration membranes: Critical review of materials, structures, and applications to water purification](#)

V Sharma, G Borkute, SP Gumfekar - Chemical Engineering Journal, 2021

14. **Abstract:** Emerging contaminants generated due to industrialization have shrunk fresh water bodies. Nanofiltration membranes are relatively efficient at separating contaminants of various sizes and functionalities. Moreover, ease of scale-up, negligible environmental footprint, and energy recovery ability make membrane filtration a future technology for complex water purification. Biomimetic or bioinspired membranes are researched to overcome the permeability-selectivity tradeoff of the existing membranes. Since biological cell membranes can selectively transport various components across membranes via aligned channels, mimicking the architecture can enable the tunable selectivity and removal of various contaminants in wastewater. This comprehensive review examines recent advances in newer materials for biomimetic membranes, their characteristics, and their application for various wastewater treatments. We also discuss various challenges such as difficulty in mimicking the exact cell structure, fouling, and stability of biomimetic materials and present opportunities for further research. We conclude that reproducible and easy processing of biomimetic materials into membranes is required for commercial applications. This review aims at a brief and systematic overview of biomimetic membranes for wastewater treatment and a description of newer materials developed to mimic the biological membranes.

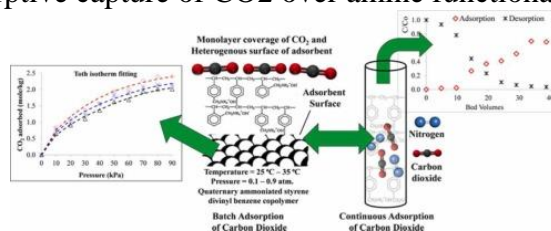
[Carbon Dioxide Capture Over Amine Functionalized Styrene Divinylbenzene Copolymer: An Experimental Batch and Continuous Studies](#)

KB Ansari, VG Gaikar, QT Trinh, MS Khan, A Banerjee... - Journal of Environmental Chemical Engineering, 2022

15.

Abstract: Cement industries are the second-largest anthropogenic carbon dioxide (CO₂) emitter and have gained substantial research attention to capture CO₂ and minimize environmental issues. Also, the recovered carbon dioxide (CO₂) can be reutilized for several applications. The adsorptive capture of CO₂ appears promising as compared to absorption, membrane separations, and cryogenic distillation because it allows easy CO₂ recovery. This work demonstrates the adsorptive capture of carbon dioxide on amine-functionalized styrene-divinylbenzene copolymer. Both batch and continuous adsorption data of CO₂ are presented at different temperatures. The equilibrium uptake of CO₂ over the polymeric adsorbent showed 2.4 mol/kg capacity at 25°C and near ambient pressure, which decreased by 16% with a ten-degree rise in the operating temperature. The equilibrium adsorption data are modeled with Langmuir, Nitta, Toth, Dubinin-Radushkevich, and SIPS isotherm equations to characterize the CO₂-polymer adsorption system and estimate the heat of adsorption, entropy, and Gibbs free energy for CO₂ adsorption. The Toth isotherm gave the best fit of the experimental data suggesting monolayer adsorption of CO₂ on energetically different sites of the adsorbent. The diffusivity of CO₂ within the adsorbent's interstitial space is determined as $2-9 \times 10^{-11}$ m²/sec, indicating intraparticle mass transfer limitations for large-scale operations. The continuous adsorption/desorption studies of CO₂ in mixtures with nitrogen were characterized via breakthrough curves. The desorption studies showed 92–94% recovery of CO₂ in batch and continuous experiments at 56°C. A theoretical model for continuous adsorption of CO₂ is also developed and validated with the experimental data. The current work could be promising for CO₂ capture in the cement industry.

Graphical Abstract: Adsorptive capture of CO₂ over amine functionalized polymeric adsorbent



[CdAgAlloy@ polymer dots of Biginelli polyamide for the highly sensitive and selective recognition of nerve agent mimics in an aqueous and vapor phase](#)

M Kaur, N Kaur, N Singh - Journal of Materials Chemistry C, 2021

16.

Abstract: In today's world, toxic nerve agents pose a significant threat to humankind, and their detection methodology requires an advanced, facile method with a rapid response that is also handy and economical. For the first time, we fabricated bimetallic CdAg alloy over a Biginelli-based non-conjugated polymer dot (Pdot) surface, with chemical reduction in water. The fabricated CdAgAlloy@Pdots were then fully characterized by the use of physicochemical techniques. The modified surface of the Pdots resulted in increased activity and selectivity, and decreased inter-Pdot distance, with generated surface conductivity towards polar organophosphates. The conductive surface was able to selectively bind polar diethylchlorophosphate (DCP) and diethylcyanophosphonate (DCNP), which are nerve agent mimics, through weak interactions such as dipole–dipole or H-bonding interaction. The sensing mechanism was demonstrated by transmission electron microscopy (TEM), FT-IR, 31P NMR images, and cyclic voltammetry (CV)

	<p>studies. The limit of detection of the sensor for DCP and DCNP was 0.85 nM and 1.2 nM, respectively. In the presence of DCP, the blue color of CdAgAlloy@Pdots changed to fluorescent greenish-yellow under UV light at 365 nm. Based on these results, we fabricated economic test paper strips for an instant, rapid, and sensitive vapor phase detection of DCP that occurred within a few seconds. Hence, we incorporated many key innovations for DCP detection into the formation of bimetallic CdAg alloy@Pdots, which possess long-term economic and sustainable features for real-world sensing applications.</p>
17.	<p>Challenges and prospects in the selective photoreduction of CO₂ to C₁ and C₂ products with nanostructured materials: a review A Behra, AK Kar, R Srivastava - <i>Materials Horizons</i>, 2021</p> <p>Abstract: Solar fuel generation through CO₂ hydrogenation is the ultimate strategy to produce sustainable energy sources and alleviate global warming. The photocatalytic CO₂ conversion process resembles natural photosynthesis, which regulates the ecological systems of the earth. Currently, most of the work in this field has been focused on boosting efficiency rather than controlling the distribution of products. The structural architecture of the semiconductor photocatalyst, CO₂ photoreduction process, product analysis, and elucidating the CO₂ photoreduction mechanism are the key features of the photoreduction of CO₂ to generate C₁ and C₂ based hydrocarbon fuels. The selectivity of C₁ and C₂ products during the photocatalytic CO₂ reduction have been ameliorated by suitable photocatalyst design, co-catalyst, defect states, and the impacts of the surface polarisation state, etc. Monitoring product selectivity allows the establishment of an appropriate strategy to generate a more reduced state of a hydrocarbon, such as CH₄ or higher carbon (C₂) products. This article concentrates on studies that demonstrate the production of C₁ and C₂ products during CO₂ photoreduction using H₂O or H₂ as an electron and proton source. Finally, it highlights unresolved difficulties in achieving high selectivity and photoconversion efficiency of CO₂ in C₁ and C₂ products over various nanostructured materials.</p>
18.	<p>Communication Quality-conscious Synthesis of 3-D Coverage using Switched Multibeam Multi-Sector Array Antenna for V2I Application S Kumar, A Sharma, S Kalra, M Kumar - <i>IEEE Transactions on Vehicular Technology</i>, 2021</p> <p>Abstract: In this paper, a switched multibeam multi-sector array antenna is proposed to provide 3-D coverage for vehicle to infrastructure (V2I) under 5G-IoT application framework. The multi-sector design is optimized using a quality-conscious communication area synthesis process to achieve 360 coverage in azimuth. Each sector of the design has two microstrip array antenna (MAA) to obtain coverage in the upper and lower halves of the elevation region. The proposed antenna is designed to enhance frequency-dependent beam squint phenomena exploited to achieve multibeam coverage in the elevation region. The simulation results of the proposed antenna having 3 2 size of MAA indicates the achieved desired radiation characteristics, and a prototype of the same operating in WLAN band (5.15 5.825 GHz) is fabricated for verification. The experimental results show the maximum realized gain is 7.85 dBi and the beam tilt of 10.8 to 46.8 in elevation is achieved at central frequencies 5.15 GHz and 5.825 GHz, respectively. The coverage obtained is 360 in azimuth and 93.6 in elevation. The signal to interference ratio is measured around the antenna, which shows interference suppression of more than 10 dB achieved between the MAAs of alternate sectors. Moreover, the port isolation is better than 26 dB. Hence, sixteen simultaneous beams utilizing frequency re-use can be operated in the 3-D space around the access point to communicate with multiple drones/vehicles and IoT nodes to realize a smart vehicular application.</p>

[Design of a Modified Single-stage and Multistage EMI Filter to Attenuate Common and Differential Mode Noise in SiC Inverter](#)

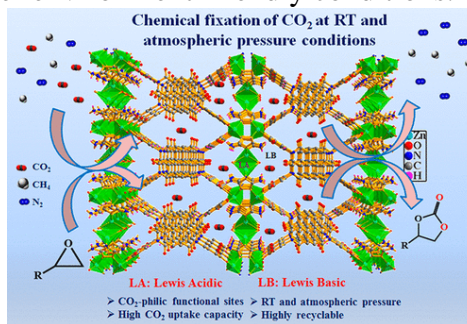
M Kumar, K Jayaraman - IEEE Journal of Emerging and Selected Topics in Power Electronics, 2021

19. **Abstract:** The SiC inverter switching at high frequencies introduce increased common-mode (CM) and differential-mode (DM) electromagnetic interference (EMI) issues such as shaft voltage, bearing currents, insulation degradation, and poor current quality in motor. These EMI issues are commonly addressed with EMI filters employing CM and DM inductor. The increased volume and poor performance of a CM inductor designed for SiC inverter switching at high frequency requires modified EMI filter design procedure for enhanced performance and volume minimization. In this work, three EMI filters are presented with modified design procedures. A single stage EMI filter is designed by incorporating a DM filter offering an equal attenuation to DM and CM noise at switching frequency. Here, the additional CM attenuation demand is fulfilled by a marginal value of CM inductor. While in multistage EMI filters, the required CM attenuation is split between the two stages. The multistage EMI filter-1 is designed using an additional CM inductor and existing load capacitance as the second-stage. Whereas, the multistage EMI filter-2 is designed with a lesser value of CM inductance to provide CM attenuation over the entire conducted EMI frequency range. The modified EMI filters are tested on a SiC inverter operating at 200 kHz.


[Design of Bifunctional Zinc \(II\)–Organic Framework for Efficient Coupling of CO₂ with Terminal/Internal Epoxides under Mild Conditions](#)

R Das, T Ezhil, CM Nagaraja - Crystal Growth & Design, 2021

20. **Abstract:** The rational design of efficient catalytic materials for conversion of carbon dioxide (CO₂), a greenhouse gas into valuable products has fascinated chemists ever since the advent of the area of green and sustainable catalysis. Herein, we report design of a bifunctional, 3D Zn-MOF, [Zn₃(BINDI)(DATRZ)₂(H₂O)₂]_n by utilizing a Lewis acidic Zn(II) ion, long-chain, rigid aromatic tetracarboxylate ligand, N,N'-bis(5-isophthalic acid)naphthalenediimide (BINDIH₄) and basic –NH₂ rich 3,5-diamino-1,2,4-triazole (DATRZ) linker. The Zn-MOF possesses a BET surface area of 1085.8 m²/g and a high density of CO₂-philic –NH₂ groups lined in the 1D channels promoting selective and recyclable CO₂ adsorption with a high heat of interaction energy of 44.3 kJ/mol. The high surface area combined with the presence of Lewis acidic (LA) and basic sites rendered Zn-MOF an ideal bifunctional heterogeneous catalyst for efficient coupling of CO₂ with terminal/internal epoxides under eco-friendly, solvent-free, RT and atmospheric pressure (balloon) conditions. Interestingly, Zn-MOF showed excellent catalytic activity for fixation of CO₂ even from simulated flue gas/dilute CO₂ gas. Remarkably, Zn-MOF showed high recyclability for up to 10 cycles with retaining the framework stability and catalytic activity. Overall, this work demonstrates the rational integration of Lewis acidic and basic sites in a 3D framework for the efficient utilization of CO₂ under environment-friendly conditions.



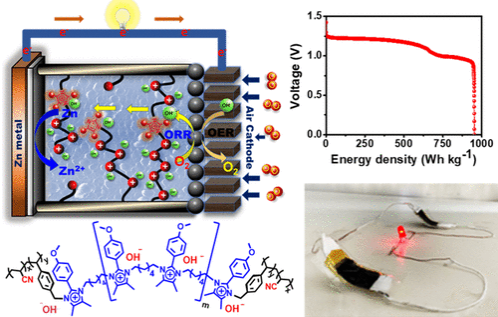
21.	<p>Does salting-out effect nucleate nanobubbles in water: Spontaneous nucleation? K Agarwal, M Trivedi, N Nirmalkar - Ultrasonics Sonochemistry, 2022</p> <p>Abstract: The solubility of gases in aqueous salt solution decreases with the salt concentration, often termed the “salting-out effect.” The dissolution of salt in water is followed by dissociation of salt and further solvation of ions with water molecules. The solvation weakens the affinity of gaseous molecules, and thus it releases the excess dissolved gas. Now it is interesting to know that what happens to the excess gas released during salting-out? Since it is imperative to note that the transfer of the dissolved gas in the bulk liquid may often occur in the form of nanobubbles. In this work, we have answered this question by investigating the nano-entities nucleation during the salting-out effect. The solubility of gases in aqueous salt solution decreases with the salt concentration, and it is often termed as the “salting-out effects.” The dissolution of salt in water undergoes dissociation of salt and further solvation of ions with water molecules. The solvation weakens the affinity of gaseous molecules, and thus it releases the excess dissolved gas. Now it is interesting to know that what happens to the excess gas released during salting-out? While it is also imperative to note that the gas transfer in the bulk liquid often occurs in the form of bubbles. With this hypothesis, we have experimentally investigated that whether the salting-out effect nucleates nanobubble or not. What is the strong scientific evidence to prove that they are nanobubbles? Does the salting-out parameter affect the number density? The answers to such questions are essential for the fundamental understanding of the origin and driving force for nanobubble generation. We have provided three distinct proofs for the nano-entities to be the nanobubbles, namely, (1) by freezing and thawing experiments, (2) by destroying the nanobubbles under ultrasound field, and (3) we also proposed a novel method for refractive index estimation of nanobubbles to differentiate them from nano drops and nanoparticles. The refractive index (RI) of nanobubbles was estimated to be 1.012 for mono- and di-valent salts and 1.305 for trivalent salt. The value of RI closer to 1 provides strong evidence of gas-filled nanobubbles. Both positive and negative charged nanobubbles nucleate during the salting-out effect depending upon the valency of salt. The nanobubbles during the salting-out effect are stable only for up to three days. This shorter stability could plausibly be due to reduced colloidal stability at a low surface charge.</p>
22.	<p>Drugs repurposed: An advanced step towards the treatment of breast cancer and associated challenges JA Malik, S Ahmed, B Jan, O Bender... - Biomedicine & Pharmacotherapy, 2021</p> <p>Abstract: Breast cancer (BC) is mostly observed in women and is responsible for huge mortality in women subjects globally. Due to the continued development of drug resistance and other contributing factors, the scientific community needs to look for new alternatives, and drug repurposing is one of the best opportunities. Here we light upon the drug repurposing with a major focus on breast cancer. BC is a division of cancer known as the leading cause of death of 2.3 million women globally, with 685,000 fatalities. This number is steadily rising, necessitating the development of a treatment that can extend survival time. All available treatments for BC are very costly as well as show side effects. This unfulfilled requirement of the anti-cancer drugs ignited an enthusiasm for drug repositioning, which means finding out the anti-cancer use of already marketed drugs for other complications. With the advancement in proteomics, genomics, and computational approaches, the drug repurposing process hastens. So many drugs are repurposed for the BC, including alkylating agents, antimetabolite, anthracyclines, an aromatase inhibitor, mTOR, and many more. The drug resistance in breast cancer is rising, so reviewing how the challenges in breast cancer can be combated with drug repurposing. This paper provides the updated information on all the repurposed drugs candidates for breast cancer with the molecular mechanism responsible for their anti-tumor activity. Additionally, all the challenges that occur during the repurposing of</p>

	<p>the drugs are discussed.</p> <p>Graphical Abstract:</p> 
23.	<p>Effect of the damping ratio of non-structural components on floor acceleration demands in torsionally irregular buildings A Jain, M Surana - 8th International Conference on Computational Methods in Structural Dynamics and Earthquake Engineering, 2021</p> <p>Abstract: To investigate the effect of damping ratio of non-structural components on floor acceleration demands in torsionally irregular buildings, reinforced-concrete moment-resisting frame buildings resting on flat ground (regular), and on hill slopes (irregular) are analyzed. Bidirectional linear dynamic analyses are conducted, by applying a suite of far-field ground motions, along two orthogonal axes, to obtain the floor response of the investigated frames. From the obtained floor acceleration response of the investigated buildings, the elastic floor response spectra are derived at two different floor levels: (i) the floor with maximum eccentricity in the irregular building, and the corresponding floor in the reference regular building; and (ii) at the roof levels, for both the regular and irregular buildings, for NSC's damping ratios of 1%, 2%, 5%, and 10%. The effect of damping ratio of the NSCs is studied in terms of damping modification factors, at three different locations on each of the considered floor levels, i.e. (i) at the flexible edge, (ii) at the center of rigidity, and (iii) at the stiff edge. The derived median damping modification factors, as obtained from the time-history analyses are compared with the recommendations of EC 8 and other existing models available in the literature. It is observed that the recommendations of EC 8 underpredict damping modification factors significantly, for non-structural components, tuned to structural modes of vibration, especially, for low damping ratios of the non-structural components, and also for relatively flexible non-structural components, for high damping ratio of the non-structural components.</p>
24.	<p>Electronic Structure Calculations and Quantum Dynamics of Rotational Deexcitation of CNNC by He S Chhabra, TJD Kumar - Physical Chemistry Chemical Physics, 2021</p> <p>Abstract: Quantum dynamics of rotational transitions of the diisocyanogen (CNNC) molecule undergoing collision with helium (He) atom occurring in the interstellar medium (ISM) has been studied. The rotational deexcitation cross sections are extracted by first computing an ab initio potential energy surface of CNNC—He using the coupled-cluster with single and double and perturbative triple excitation with F12a method (CCSD(T)-F12a) employing aug-cc-pVTZ basis set. Utilizing the multipole expansions, collisional cross sections have been determined for total energies up to 1000 cm⁻¹ by the close coupling equations. The discussion on propensity rules suggests that the transitions have even Δj value, while odd Δj valued transitions are forbidden due to C and N nuclei spin statistics. Quasi-bound states present in the CNNC—He van der Waals complex resulted in the resonances coming from the rapid oscillation in the value of cross sections in the region of low energy. Rotational deexcitation rate coefficients are further worked out by</p>

	averaging the calculated cross sections at temperatures below 200K. The new findings of the study will be beneficial in modeling the abundance of diisocyanogen in ISM.
25.	<p>Enhanced Condensation on Soft Materials through Bulk Lubricant Infusion CS Sharma, A Milionis, A Naga, CWE Lam... - <i>Advanced Functional Materials</i>, 2021</p> <p>Abstract: Soft substrates enhance droplet nucleation during water vapor condensation because their deformability inherently reduces the energetic threshold for heterogeneous nucleation relative to rigid substrates. However, this enhancement is counteracted later in the condensation cycle, when substrate viscoelastic dissipation inhibits condensate droplet shedding. Here a polydimethylsiloxane (PDMS) based organogel is designed to overcome this limitation. It is shown that merely 5% bulk lubricant infusion in PDMS reduces viscoelastic dissipation in the substrate by nearly 28 times while doubling the droplet nucleation density. Parameters for water condensation on this organogel are correlated with material properties controlled by design, i.e., fraction and composition of uncrosslinked chains and shear modulus. It is demonstrated that the increase in nucleation density and reduction in precoalescence droplet growth rate is rather insensitive to the lubricant percentage in PDMS within the broad range investigated. These results indicate the presence of a lubricant layer on the substrate surface that cloaks the growing condensate droplets. This cloaking effect is visualized, and it is shown that cloaking occurs significantly faster on PDMS if it is infused with bulk lubricant. Overall, bulk lubricant infusion in PDMS enhances condensation and leads to a more than 40% higher dewing on the substrate.</p>
26.	<p>Hydrolysis and Condensation of Tetraethyl Orthosilicate at the Air–Aqueous Interface: Implications for Silica Nanoparticle Formation H Kaur, S Chaudhary, H Kaur, M Chaudhary, KC Jena - <i>ACS Applied Nano Materials</i>, 2021</p> <p>Abstract: The silica (SiO₂) nanoparticles of a well-known silica precursor tetraethyl orthosilicate (TEOS) are generally synthesized via a promising solution-gelation inorganic polymerization process. The monodisperse silica nanoparticles have potential applications ranging from the formation of dental nanocomposites to antireflective coatings. In the present study, we have systematically investigated the in situ interfacial molecular structure of TEOS and its impact on the interfacial water structure during the processes of hydrolysis and condensation at the air–aqueous interface using sum-frequency generation (SFG) vibrational spectroscopy. With the presence of water, a gradual decrease in the SFG intensity in the CH-stretch region for each concentration of TEOS with time reflects the elimination of ethoxy groups, which is a signature of the hydrolysis process. Further, the impact of the hydrolysis process is revealed from the significant enhancement in the SFG signal in the OH-stretch region. The hydrolysis of TEOS is then followed by condensation in which the $\equiv\text{Si}-\text{O}^-$ charged species are replaced by forming the $\equiv\text{Si}-\text{O}-\text{Si}\equiv$ bridging network. The signature of the condensation process is reflected with the gradual decrease in the observed enhanced SFG signal in the OH-stretch region. The formation of monodispersed silica nanoparticles as an end product of size variation from 1.75 to 4.67 nm with the increase in TEOS concentration is confirmed with the DLS measurements. We have also probed the pH-dependent SFG studies at three different pH values (2.0, 5.8, and 9.0). The dominant pH-dependent hydrolysis process is revealed from the observed molecular structure of TEOS at the air–aqueous interface.</p>

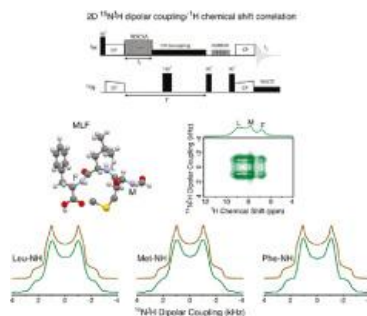
27.	<p>Influence of Cold Spray Parameters on Bonding Mechanisms: A Review S Singh, RK Raman, CC Berndt, H Singh - Metals, 2021</p> <p>Abstract: The cold spray process is governed by the impact of high velocity feedstock particles onto a substrate without melting. Hence, the bulk material properties are retained. However, it is challenging to achieve good adhesion strength. The adhesion strength depends on factors such as the cold spray process parameters, substrate conditions, coating/substrate interactions at the interface and feedstock material properties. This review examines fundamental studies concerning the adhesion mechanisms of cold spray technology and considers the effect of cold spray input parameters such as temperature, stand-off-distance, pressure, process gas, spray angle, and traverse speed of the cold spray torch on the bonding mechanism and adhesion strength. Furthermore, the effects of substrate conditions such as temperature, hardness, roughness and material on the adhesion mechanism are highlighted. The effect of feedstock properties, such as feed rate, shape and size are summarized. Understanding the effect of these parameters is necessary to obtain the optimal input parameters that enable the best interfacial properties for a range of coating/substrate material combinations. It is expected that feedstock of spherical morphology and small particle size (<15 μm) provides optimal interfacial properties when deposited onto a mirror-finished substrate surface using high pressure cold spray. Deep insights into each parameter exposes the uncovered potential of cold spray as an additive manufacturing method.</p>
28.	<p>Interacting Shell Model Calculations for Neutrinoless Double Beta Decay of ^{82}Se With Left-Right Weak Boson Exchange Y Iwata, S Sarkar - Frontiers in Astronomy and Space Sciences, 2021</p> <p>Abstract: In the present work, the λ mechanism (left-right weak boson exchange) and the light neutrino-exchange mechanism of neutrinoless double beta decay is studied. In particular, much attention is paid to the calculation of nuclear matrix elements for one of the neutrinoless double beta decaying isotopes ^{82}Se. The interacting shell model framework is used to calculate the nuclear matrix element. The widely used closure approximation is adopted. The higher-order effect of the pseudoscalar term of nucleon current is also included in some of the nuclear matrix elements that result in larger Gamow-Teller matrix elements for the λ mechanism. Bounds on Majorana neutrino mass and lepton number violating parameters are also derived using the calculated nuclear matrix elements.</p>
29.	<p>Kashmiri Hamam: An Exploration of Technical Design Within Traditional Architecture and Culture S Sakinah, M Hamid, P Chopra, AA Baba, AH Sahir... - IEEE Global Humanitarian Technology Conference, 2021</p> <p>Abstract: Hamam is a culturally important architectural feature of homes and mosques in the Kashmir Valley of India that has deep roots in Islamic religion and culture. Culturally, Hamam is a gathering place for families and visitors, and a space for individuals to participate in prayer and purification rituals. Functionally, Hamam is a room within a home in which the subfloor is hollow</p>

	<p>and is comprised of a wood-fired furnace to generate heat which is conducted through the floor, warming the space and occupants in the Hamam. Trained Kashmiri artisans construct and maintain the Hamam according to longstanding traditions. The Hamam is one of several traditional means that Kashmiris use for space and self heating during the winter season. This paper investigates the needs and preferences of Hamam users through mixed-method interviews, computational modeling and physical measurement. The results of this research include household needs and preference regarding their Hamam, and measurements and MATLAB simulation to characterize the thermal behavior of Hamam. The methods used included installing specific temperature and humidity sensors to record the temperature and then comparing the results with the help of MATLAB.</p>
30.	<p>Neutron transfer in $^9\text{Be} + ^{159}\text{Tb}$ system M Kaushik, G Gupta, VV Parkar, SK Pandit, S Thakur... RG Pillay... PP Singh - The European Physical Journal A, 2021</p> <p>Abstract: One neutron stripping cross sections (σ_{-1n}) are measured in $^9\text{Be} + ^{159}\text{Tb}$ system in the energy range $E_{\text{cm}}/V_B \sim 0.79\text{--}1.24$ using offline gamma counting technique. The CRC model calculations including the ground state and the 2+ resonance state of ^8Be, carried out using the FRESKO code, give a reasonable description of the measured data. In addition, comparisons of reduced 1n-stripping cross sections- σ_{red} with ^9Be for different target nuclei ($A \sim 150\text{--}200$), and σ_{red} for ^9Be, ^6Li with ^{159}Tb target are presented. While no strong target dependence is observed with ^9Be projectile, $\sigma_{\text{red}}(^9\text{Be})$ is significantly larger than that for ^6Li, which is consistent with the Q-value for transfer reactions and breakup threshold energy of projectiles.</p>
31.	<p>New remains of Nalamera (Tragulidae, Mammalia) from the Ladakh Himalaya and their phylogenetical and palaeoenvironmental implications B Mennecart, WA Wazir, RK Sehgal, R Patnaik... N Kumar... - Historical Biology, 2021</p> <p>Abstract: Nalamera savagei is one of the rare mammals found in India during the Oligocene. Five dental remains composed the originally found material, described in 1990. The first phylogenetic hypothesis proposed Nalamera to be closely related to the basal ruminant Lophiomerycidae. The description of new specimens from the type bed K/7b from the Kargil Formation (late Oligocene, India), led to a reinterpretation of the phylogenetic position of Nalamera and of the early evolutionary history of the Tragulidae. Based on our phylogenetic hypothesis, Nalamera is nested within the living Tragulidae, making it one of the oldest known tragulid. Moreover, the enigmatic late Eocene Stenomeryx from Myanmar is not recovered as a ruminant in our analysis. Tooth isotopic data indicate that Nalamera fed on plants that have grown under xeric conditions. This is in agreement with palaeoenvironmental information observed on plants from Turkish and Pakistani localities where Nalamera has already been found. This region of the world had a seasonal climate with an arid period during the late Oligocene.</p>
32.	<p>Onset of flow reversal in a vertical T-channel: Bingham fluids A Maurya, N Tiwari, RP Chhabra - Chemical Engineering & Technology, 2021</p> <p>Abstract: This work investigates the commencement of the flow reversal phenomenon which occurs in the daughter branch of a vertical T-channel for the flow of Bingham plastic fluids. The combined influences of the imposed forced flow and buoyancy-driven flow have been analysed at low Reynolds numbers. The mixed convection flow of a Bingham model fluid is explored for a wide range of conditions as: Prandtl number ($1 \leq \text{Pr} \leq 50$), Richardson number ($0 \leq \text{Ri} \leq 4$) and Bingham number ($0.01 \leq \text{Bn} \leq 20$). Results show that the critical Richardson number is strongly influenced by Pr and the yield stress of the Bingham fluids. The dimensionless pressure is seen to decrease with the critical Richardson number. Also, the fractional flow passing through the main branch exhibits a strong direct dependence on the Richardson number while an opposite</p>

	relationship with Bn and Pr.
33.	<p>Pendent Persubstituted Imidazolium and a Polyimidazolium Cross-Linked Polymer as Robust Alkaline Anion Exchange Membranes for Solid-State Zn–Air Batteries G Singh, M Kumar, TS Thomas, TC Nagaiah, D Mandal - ACS Applied Energy Materials, 2021</p> <p>Abstract: Alkaline anion exchange membranes (AEMs) were developed from a series of persubstituted imidazolium cations with varying alkyl chains (Im-<i>n</i>C, <i>n</i>C = (CH₂)_{<i>n</i>–1}CH₃; <i>n</i> = 4, 12, and 16) tethered on poly(vinylbenzyl chloride-co-acrylonitrile) (PVC-co-AN) to prepare a comb-shaped polymer membrane (M1-<i>n</i>C) and a cross-linked polymer membrane from polyimidazolium cations and PVC-co-AN (M₃). The PVC-co-AN polymer backbone shows high stability after curing, and the water uptake and swelling ratio are controlled by varying the alkyl chain length in M1-<i>n</i>C even with temperature variation. Results show that M1-16C retains the highest ion exchange capacity (IEC) of 95% among the M1-<i>n</i>C series of membranes after exposure to 1 M KOH solution at 80 °C for 30 days. However, the longer alkyl chains hindered the interconnected ion channels limiting the hydrophobic/hydrophilic phase separation and the hydroxide ion conductivity. Meanwhile, M3 exhibits a distinct microphase-separated morphology and a high ionic conductivity of 54.5 mS/cm for a 2.02 IEC with high stability to retain an IEC of 97% after storage in 1 M KOH solution at 80 °C for 30 days. In addition, all the AEMs exhibit high oxidation stability and retain >96% weight after immersion into 4 ppm Fenton’s reagent at 80 °C. Moreover, the flexible solid-state zinc–air batteries comprising an M3 membrane displayed a peak power density of 165 mW cm^{–2} and superior cycling stability (30 h at 10 mA cm^{–2}) demonstrating very promising applications in solid-state flexible rechargeable Zn–air batteries.</p> 
34.	<p>Polymer-based self-assembled photonic crystals to tune the light transport and emission P Priya, SK Saini, R Nair - Chemical Communications, 2022</p> <p>Abstract: The advent of photonic crystals has materialized the idea of taming the flow of light which has revolutionized the photonics technology. Photonic crystals are constructed by the periodic variation of refractive index in one-, two-, or three-spatial dimensions on an optical wavelength scale. Photonic crystals are inherited with photonic stop gaps or band gaps depending upon the crystal symmetry and refractive index contrast. With an ease of fabrication, polymer-based self-assembled photonic crystals with stop gaps are widely explored. We discuss the angle- and polarization-dependent stop gaps creation and their splitting at higher angles of incidence. The observed stop gaps in self-assembled photonic crystals are often deviate from the theoretical predictions due to experimental constraints such as the finite-size and fabrication disorders associated with sample. We perform micro-reflectivity experiments on a single domain, which show minimal disorder, with nearly 100% reflectivity in agreement with theory. We obtain more than 75% emission intensity suppression and a 30% increase in the emission lifetime at the stop gap using the micro-emission experiment from the single domain. This enable us to study the role of finite-size effects in photonic crystals in modifying the emission properties. We observe a linear</p>

	scaling of the emission intensity suppression as well as the emission rate with finite-size of the crystal. Our single-domain experimental studies reveal that low-index contrast self-assembled photonic crystals is a potential platform to strategically modify the light transport and emission properties.
35.	<p>Process variation aware DRAM-cache resizing B Agarwalla, S Das, N Sahu - Journal of Systems Architecture, 2021</p> <p>Abstract: As the demand for larger-sized Last Level Cache (LLC) grows due to modern data-intensive applications, employing low-density SRAM technology to create the LLC for the multicore system is no longer advantageous. Because capacity is more essential than latency in LLC, employing high-density DRAM technology to design LLC is an alternative approach. However, in order to employ DRAM as an LLC, several of its fundamental disadvantages must be effectively addressed. The DRAM-LLC is typically used in die-stacking technology, where the LLC is layered on top of the core layer. The LLC is also separated into several banks. Though larger-sized LLCs are preferred for data-intensive applications, they are not required for all applications. To lower the energy consumption of DRAM-LLC, the size of the LLC can be reduced by shutting down some unused component (bank) of the LLC. These powered-off banks can be reopened whenever the LLC capacity is increased. LLC resizing is the name of the procedure. Because of manufacturing variance, the entire DRAM-LLC does not react evenly. The section affected by process variation has higher delay and energy consumption than the other portions. In this paper, we propose a Process Variation Aware LLC Resizing (PVAR), in which the shrinkage is accomplished by shutting down the affected banks. The existing resizing strategies primarily target underused banks, but these underused banks may be healthy, and instead of powering down these banks, powering down the affected bank is more useful. Experiment results demonstrate that the suggested LLC resizing reduces energy usage by up to 47% more than existing solutions.</p>
36.	<p>Proton-detected ^{15}N-^1H dipolar coupling/^1H chemical shift correlation experiment for the measurement of NH distances in biological solids under fast MAS solid-state NMR E Nehra, N Sehrawat, T Kobayashi, Y Nishiyama, MK Pandey - Journal of Magnetic Resonance Open, 2021</p> <p>Abstract: Measurement of distances from dipolar couplings is essential for structural characterization, refinement and validation using the solid-state nuclear magnetic resonance (ssNMR) spectroscopy. Particularly, knowledge about NH dipolar interactions in biological solids is important for understanding the hydrogen (H)-bonding interactions, molecular geometry and spin dynamics. In this regard, we have proposed a proton-detected two-dimensional (2D) ^{15}N-^1H dipolar coupling/^1H chemical shift correlation experiment using the C-symmetry based windowless recoupling of chemical shift anisotropy (ROCSA) in combination with the DIPSHIFT pulse-based method for the measurement of short NH distances in the isotopically labeled and naturally abundant biological solids at fast magic angle spinning (MAS) rates (40–70 kHz). Our proposed method results in undistorted recoupled ^{15}N-^1H dipolar coupling powder lineshapes that are free from the recoupled ^1H CSA contributions under the ^{15}N evolution, a feature that is essential for the measurement of NH distances with improved accuracy (± 500 Hz in terms of the NH dipolar couplings). The pulse sequence developed in the present study is also insensitive to the ^1H-^1H homonuclear dipolar interactions, relaxation effects owing to its constant-time implementation, and t_1-noise from the fluctuations in the MAS.</p>

Graphical Abstract:



[Quantum Dynamics of Rotational Transitions in CN \(\$X^2\Sigma^+\$ \) by \$H^+\$ Collisions](#)

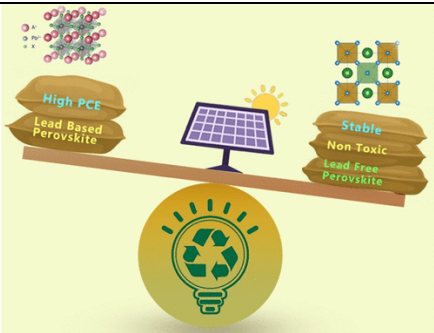
[B Anusuri, TJD Kumar, S Kumar - Frontiers in Chemistry, 2021](#)

37. **Abstract:** Collisional cross-sections of inelastic rotational excitations of CN in its ground electronic state ($X^2\Sigma^+$) by H^+ scattering are studied by the exact quantum mechanical close-coupling (CC) method at very low collision energies ($0\text{--}600\text{ cm}^{-1}$) relevant to interstellar atmospheres. Ab initio rigid rotor potential energy surface computed at MRCI/cc-pVTZ level of accuracy has been employed. Rate coefficients for the rotational excitations have also been calculated. The obtained results are compared with previous theoretical calculations and analyzed whether proton collisions could be significant sources for rotationally excited CN as a possible source for cosmic microwave background of about 3 K from the interstellar media.

[Recent Advancements in Nontoxic Halide Perovskites: Beyond Divalent Composition Space](#)

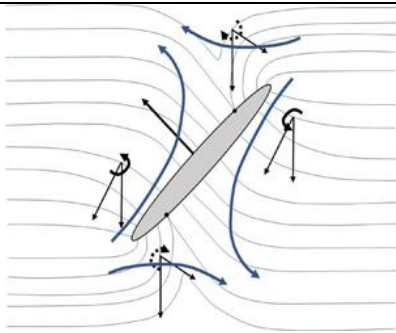
[D Kumar, J Kaur, PP Mohanty, R Ahuja, S Chakraborty - ACS Omega, 2021](#)

38. **Abstract:** Since the inception of organic–inorganic hybrid perovskites of ABX_3 stoichiometry in 2009, there has been enormous progress in envisaging efficient solar cell materials throughout the world, from both the theoretical and experimental perspectives. Despite achieving 25.5% efficiency, hybrid halide perovskites are still facing two main challenges: toxicity due to the presence of lead and device stability. Two particular families with $A_3B_2X_9$ and $A_2MM'X_6$ stoichiometries have emerged to address these two prime concerns, which have restrained the advancement of solar energy harvesting. Several investigations, both experimental and theoretical, are being conducted to explore the holy-grail materials, which could be optimum for not only efficient but also stable and nontoxic photovoltaics technology. However, the trade-off among stability, efficiency, and toxicity in such solar energy materials is yet to be completely resolved, which requires a systematic overview of $A_3B_2X_9$ - and $A_2MM'X_6$ -based solar cell materials. Therefore, in this timely and relevant perspective, we have focused on these two particular promising families of perovskite materials. We have portrayed a roadmap projecting the recent advancements from both theoretical and experimental perspectives for these two exciting and promising solar energy material families while amalgamating our critical viewpoint with a future outlook.

	
39.	<p>Recent advances in low-cost, portable automated resuscitator systems to fight COVID-19 V Kumar, R Kumar, M Kumar, GS Wander, V Gupta, Ashish Sahani - Health and Technology, 2021</p> <p>Abstract: World is fighting one of its greatest battle against COVID-19 (a highly infectious disease), leading to death of hundreds of thousands of people around the world, with severe patients requiring artificial breathing. To overcome the shortage of ventilators in medical infrastructure, various low-cost, easy to assemble, portable ventilators have been proposed to fight the ongoing pandemic. These mechanical ventilators are made from components that are generally readily available worldwide. Such components are already associated with day-to-day gadgets or items and which do not require specialized manufacturing processes. Various designs have been proposed, focussing on meeting basic requirements for artificial ventilation to fight the ongoing pandemic. But some people are against the usage of these mechanical ventilators in real-life situations, owing to poor reliability and inability of these designs to meet certain clinical requirements. Each design has its own merits and demerits, which need to be addressed for proper designing. Therefore, this article aims to provide readers an overview of various design parameters that needs to be considered while designing portable ventilators, by systematic analysis from available pool of proposed designs. By going through existing literature, we have recognized multiple factors influencing device performance and how these factors need to be considered for efficient device operation.</p>
40.	<p>Recurrent Generalization of F-Polynomials for Virtual Knots and Links A Gill, M Ivanov, M Prabhakar, A Vesnin - Symmetry, 2022</p> <p>Abstract: F-polynomials for virtual knots were defined by Kaur, Prabhakar and Vesnin in 2018 using flat virtual knot invariants. These polynomials naturally generalize Kauffman's affine index polynomial and use smoothing in the classical crossing of a virtual knot diagram. In this paper, we introduce weight functions for ordered orientable virtual and flat virtual links. A flat virtual link is an equivalence class of virtual links with respect to a local symmetry changing a type of classical crossing in a diagram. By considering three types of smoothing in classical crossings of a virtual link diagram and suitable weight functions, there is provided a recurrent construction for new invariants. It is demonstrated by explicit examples that newly defined polynomial invariants are stronger than F-polynomials.</p>
41.	<p>Retrospective Analysis of Antimicrobial Susceptibility of Uropathogens Isolated from Pediatric Patients in Tertiary Hospital at Al-Baha Region, Saudi Arabia MA Alzahrani, HHM Sadoma, S Mathew, S Alghamdi, JA Malik... - Healthcare, 2021</p> <p>Abstract: Introduction: Prompt diagnosis and initiation of treatment are essential in preventing long-term renal scarring. However, increasing antibiotic resistance may delay the initiation of appropriate therapy. Methodology: A retrospective chart review was performed for patients</p>

	<p>admitted to the pediatric department with urinary tract infection (UTI) diagnosis in a large tertiary care hospital in Al Baha, Saudi Arabia, from May 2017 to April 2018. The study included children of both sexes under the age of 14 years. Results: Out of 118 urinary bacterial samples, Escherichia coli was the main etiologic agent in the community- and hospital-acquired infections. The infection rate was higher in girls (68.64%) than in boys (31.36%). The commonest isolates were Escherichia coli (44.07%), extended-spectrum beta-lactamase-producing Escherichia coli (11.86%), Klebsiella pneumoniae (9.32%), Enterococcus faecalis (7.63%), methicillin-resistant Staphylococcus epidermidis (4.24%), and coagulase-negative Staphylococci (3.39%). The current study demonstrates that nitrofurantoin (19%) was the most commonly prescribed medication in the inpatient and outpatient departments, followed by trimethoprim/sulfamethoxazole (16%), amoxicillin/clavulanic acid (15%), cefuroxime (10%), azithromycin (8%), ceftriaxone (7%), and ciprofloxacin (4%), while amikacin, amoxicillin, ampicillin, cefepime, imipenem, phenoxymethylpenicillin were prescribed less commonly due to the high resistance rate. Conclusion: The microbial culture and sensitivity of the isolates from urine samples should be routine before starting antimicrobial therapy. Current knowledge of the antibiotic susceptibility patterns of uropathogens in specific geographical locations is essential for choosing an appropriate empirical antimicrobial treatment rather than reliance on recommended guidelines.</p>
42.	<p>Selective electrochemical production of hydrogen peroxide from reduction of oxygen on mesoporous nitrogen containing carbon S Mehta, D Gupta, T C. Nagaiah – ChemElectroChem, 2021</p> <p>Abstract: Heteroatom doped carbon materials with mesoporous are active catalysts to bring about oxygen reduction reaction in alkaline media. Here, we aim to see the sights of mesoporous-nitrogen containing carbon (MNC) prepared at three different temperature towards selective hydrogen peroxide (H_2O_2) production during oxygen reduction reaction in neutral media. A high H_2O_2 selectivity of 85% at 0.7 V vs. RHE is apparent with a large H_2O_2 production rate of 9.16 mmol g catalyst⁻¹ h⁻¹ and faradaic efficiency of 88.7% for MNC-600 in 0.1 M KHCO₃ solution. The effect of electrolyte towards selectivity is also premeditated. In the end, to visualize the local H_2O_2 production sequential chronoamperometry in SG-TC mode was performed using Pt-microelectrode at applied substrate potentials.</p>
43.	<p>Smoothed floating node method for modelling 2D arbitrary crack propagation problems U Singh, S Kumar, B Chen - Theoretical and Applied Fracture Mechanics, 2021</p> <p>Abstract: In this work, Floating Node Method (FNM), first developed for fracture modelling of laminate composites, is coupled with cell-wise strain Smoothed Finite Element Method (SFEM) for modelling 2D linear elastic fracture mechanics problems. The proposed method is termed as Smoothed Floating Node Method (SFNM). In this framework, FNM is used to represent the kinematics of crack and the crack front inside the domain without the requirement of remeshing and discontinuous enrichment functions during crack growth. For smoothing, a constant smoothing function is considered over the smoothing domains through which classical domain integration changes to line integration along each boundary of the smoothing cell, hence derivative of shape functions are not required in the computation of the field gradients. The values of stress intensity factor are obtained from the SFNM solution using domain based interaction integral approach. Few standard fracture mechanics problems are considered to check the accuracy and effectiveness of the proposed method. The predictions obtained with the proposed framework improves the convergence and accuracy of the results in terms of the stress intensity factors and energy norms.</p>

44.	<p>Stacked metasurfaces for enhancing the emission and extraction rate of single nitrogen-vacancy centers in nanodiamond M Khokhar, N Singh, RV Nair - Journal of Optics, 2021</p> <p>Abstract: Dielectric metasurfaces with unique possibilities of manipulating light-matter interaction lead to new insights in exploring spontaneous emission control using single quantum emitters. Here, we study the stacked metasurfaces in one- (1D) and two-dimensions (2D) to enhance the emission rate of a single quantum emitter using the associated optical resonances. The 1D structures with stacked bilayers are investigated to exhibit Tamm plasmon resonance optimized at the zero phonon line (ZPL) of the negative nitrogen-vacancy (NV-) center. The 2D stacked metasurface comprising of two-slots silicon nano-disks is studied for the Kerker condition at ZPL wavelength. The far-field radiation plots for the 1D and 2D stacked metasurfaces show an increased extraction efficiency rate for the NV- center at ZPL wavelength that reciprocates the localized electric field intensity. The modified local density of optical states results in large Purcell enhancement of 3.8 times and 25 times for the single NV- center integrated with 1D and 2D stacked metasurface, respectively. These results have implications in exploring stacked metasurfaces for applications such as single photon generation and CMOS compatible light sources for on-demand chip integration.</p>
45.	<p>The rotation of a sedimenting spheroidal particle in a linearly stratified fluid AK Varanasi, NK Marath, G Subramanian - Journal of Fluid Mechanics, 2022</p> <p>Abstract: We derive analytically the angular velocity of a spheroid, of an arbitrary aspect ratio κ, sedimenting in a linearly stratified fluid. The analysis demarcates regions in parameter space corresponding to broadside-on and edgewise settling in the limit $Re, Ri_v \ll 1$, where $Re = \rho_0 U L / \mu$ and $Ri_v = \gamma L^3 g / \mu U$, the Reynolds and viscous Richardson numbers, respectively, are dimensionless measures of the importance of inertial and buoyancy forces relative to viscous ones. Here, L is the spheroid semi-major axis, U an appropriate settling velocity scale, μ the fluid viscosity and γ (>0) the (constant) density gradient characterizing the stably stratified ambient, with the fluid density ρ_0 taken to be a constant within the Boussinesq framework. A reciprocal theorem formulation identifies three contributions to the angular velocity: (1) an $O(Re)$ inertial contribution that already exists in a homogeneous ambient, and orients the spheroid broadside-on; (2) an $O(Ri_v)$ hydrostatic contribution due to the ambient stratification that also orients the spheroid broadside-on; and (3) a hydrodynamic contribution arising from the perturbation of the ambient stratification whose nature depends on Pe; $Pe = UL/D$ being the Péclet number with D the diffusivity of the stratifying agent. For $Pe \ll 1$, this contribution is $O(Ri_v)$ and orients prolate spheroids edgewise for all κ (>1). For oblate spheroids, it changes sign across a critical aspect ratio $\kappa_c \approx 0.41$, orienting oblate spheroids with $\kappa < \kappa_c$ edgewise and those with $\kappa > \kappa_c$ broadside-on. For $Pe \ll 1$, the hydrodynamic component is always smaller in magnitude than the hydrostatic one, so a sedimenting spheroid in this limit always orients broadside-on. For $Pe \gg 1$, the hydrodynamic contribution is dominant, being $O(Ri_v^{2/3})$ in the Stokes stratification regime characterized by $Re \ll Ri_v^{1/3}$, and orients the spheroid edgewise regardless of κ. Consideration of the inertial and large-Pe stratification-induced angular velocities leads to two critical curves which separate the broadside-on and edgewise settling regimes in the $Ri_v/Re^{3/2} - \kappa$ plane, with the region between the curves corresponding to stable intermediate equilibrium orientations. The predictions for large Pe are broadly consistent with observations.</p>

	
46.	<p>Tool Wear Behavior in μ-turning of Nimonic 90 Under Vegetable Oil-Based Cutting Fluid J Airao, H Kishore, CK Nirala - Journal of Micro and Nano-Manufacturing, 2021</p> <p>Abstract: The characteristics such as high hardness and shear modulus, low thermal conductivity, strain hardening of Nickel-based superalloys lead to high machining forces and temperature, poor surface quality and integrity, rapid tool wear, etc. The present article investigates the tool wear mechanism of the tungsten carbide (WC) tool in μ-turning of Nimonic 90 under dry, wet, and vegetable oil-based cutting fluid (VCF). Canola oil is used as vegetable oil. Three different combinations of cutting speed, feed rate, and depth of cut are considered for analysis. The tool wear is characterized using optical and scanning electron microscopy. Machining with VCF shows an approximate reduction of flank wear width in the range of 12%-52% compared to dry and wet conditions. The main wear mechanisms observed on the tool flank and rake face are abrasion, built-up edge adhesion, and edge chipping. The VCF considerably reduces the adhesion and abrasion and, hence, increases tool life. The chips produced in dry conditions are found fractured and uneven, whereas, it had an uneven lamella structure in wet conditions. The VCF found reducing the plastic deformation in each cutting condition, as a result, producing fine lamella structured chips.</p>
47.	<p>Transmitting Photons for Humanity RV Nair - Resonance, 2021</p> <p>Abstract: In this article, we recount the scientific contributions of Dr Narinder Singh Kapany and the consequent advancements in optical fiber-based technology. He is acknowledged as the “man who bent light” and the first to coin the term—‘fiber optics’. We will discuss the fiber endoscope, also known as the flexible fiberscope, which was designed by him. The properties of light on which Kapany’s work was based are elaborated. Different types of optical fibers with their distinct features and state-of-the-art developments in the field of fiber optics are also discussed.</p>

Disclaimer: This publication digest may not contain all the papers published. Library has compiled the publication data as per the alerts received from Scopus and Google Scholar for the affiliation “Indian Institute of Technology Ropar” for the month of December 2021. The author(s) are requested to share their missing paper(s) details if any, for the inclusion in the next publication digest.